JOURNAL OF VIROLOGY, Sept. 2005, p. 11476–11486 Vol. 79, No. 17
0022-538X/05/$08.00+0 doi:10.1128/JVI.79.17.11476–11486.2005

The Severe Acute Respiratory Syndrome Coronavirus Nucleocapsid Protein Is Phosphorylated and Localizes in the Cytoplasm by 14-3-3-Mediated Translocation

Milan Surjit,[1] Ravinder Kumar,[1] Rabi N. Mishra,[2] Malireddy K. Reddy,[2] Vincent T. K. Chow,[3] and Sunil K. Lal[1]*

Virology Group[1] and Plant Molecular Biology Group,[2] International Centre for Genetic Engineering & Biotechnology, Aruna Asaf Ali Road, New Delhi 110067, India, and Human Genome Laboratory, Microbiology Department, Faculty of Medicine, National University of Singapore, Kent Ridge, Singapore 117597[3]

Received 14 December 2004/Accepted 19 May 2005

The severe acute respiratory syndrome coronavirus(SARS-CoV) nucleocapsid (N) protein is one of the four structural proteins of the virus and is predicted to be a 46-kDa phosphoprotein. Our in silico analysis predicted N to be heavily phosphorylated at multiple residues. Experimentally, we have shown in this report that the N protein of the SARS-CoV gets serine-phosphorylated by multiple kinases, in both the cytoplasm and the nucleus. The phosphoprotein is stable and localizes in the cytoplasm and coprecipitates with the membrane fraction. Also, using specific inhibitors of phosphorylation and an in vitro phosphorylation assay, we show that the nucleocapsid protein is a substrate of cyclin-dependent kinase (CDK), glycogen synthase kinase, mitogen-activated protein kinase, and casein kinase II. Further, we show that the phosphorylated protein is translocated to the cytoplasm by binding to 14-3-3 (tyrosine 3-monooxygenase/tryptophan 5-monooxygenase activation protein). 14-3-3 proteins are a family of highly conserved, ubiquitously expressed eukaryotic proteins that function primarily as adapters that modulate interactions between components of various cellular signaling and cell cycle regulatory pathways through phosphorylation-dependent protein-protein interactions. Coincidentally, the N protein was also found to downregulate the expression of the theta isoform of 14-3-3 (14-3-3θ), leading to the accumulation of phosphorylated N protein in the nucleus, in the absence of growth factors. Using short interfering RNA specific to 14-3-3θ we have inhibited its expression to show accumulation of phosphorylated N protein in the nucleus. Thus, the data presented here provide a possible mechanism for phosphorylation-dependent nucleocytoplasmic shuttling of the N protein. This 14-3-3-mediated transport of the phosphorylated N protein and its possible implications in interfering with the cellular machinery are discussed.

A novel coronavirus has been associated with a worldwide outbreak of atypical pneumonia referred to as severe acute respiratory syndrome coronavirus (SARS-CoV) (1–2). SARS-CoV has exhibited a high mortality rate in infected people and has spurred intense research efforts around the world to deal with the serious threat to mankind posed by this novel coronavirus. To date more than 8,000 people have been infected, 800 are dead, and mortality rates reaching over 40% in certain populations have been documented (5).

SARS-CoV is a positive-sense, single-stranded RNA virus with ~30,000 nucleotides, which are organized into approximately 14 open reading frames, taking into consideration only those exceeding 50 amino acids in translational capacity (12, 15). Like other known coronaviruses, SARS-CoV is an enveloped virus containing three outer structural proteins, the membrane, envelope, and spike proteins. The nucleocapsid (N) protein, together with the viral RNA genome, presumably forms a helical core located within the viral envelope. The SARS-CoV nucleocapsid protein contains 423 amino acids and has been predicted to be a phosphoprotein of 46 kDa (12) and a nucleic acid binding protein and also postulated to be involved in viral transcription and replication (6). Recently, our lab has shown that this protein is capable of self-association to form dimers (19) and can induce programmed cell death and actin reorganization in mammalian cells under stress (18).

In this report we have studied the ability of the N protein to be phosphorylated in COS-1 and human hepatoma (Huh-7) cells. We have been able to show that the majority of phosphorylation occurs at the serine residues and the phosphorylated N protein localizes predominantly in the cytoplasm and associates with the membrane. Further, we provide evidence for phosphorylation-dependent 14-3-3 binding which may enable N to be efficiently transported from the nucleus to the cytoplasm. Interestingly, we have also observed downregulation of 14-3-3θ transcript levels in N-expressing cells in the absence of growth factors, leading to an accumulation of the N protein in the nucleus. Finally, inhibition of 14-3-3θ expression using short interfering RNA (siRNA) specific for it resulted in significantly increased nuclear localization of the N protein. Hence, we postulate that under different cellular conditions, interplay between these two proteins may regulate the intracellular localization of the N protein.

* Corresponding author. Mailing address: Virology Group, International Centre for Genetic Engineering & Biotechnology, P.O. Box 10504, Aruna Asaf Ali Road, New Delhi 110067, India. Phone: 91-11-26177357. Fax: 91-11-26162316. E-mail: sunillal@icgeb.res.in.

MATERIALS AND METHODS

Plasmids and reagents. The pCDNA3.1 Myc N construct and pCDNA3.1 Myc only (mock) was used in all the experiments. The N gene cloning has been described earlier (18). The green fluorescent protein (GFP) siRNA was obtained

from Vijay Kumar. The 14-3-3θ siRNA expression plasmid was constructed by cloning the 14-3-3θ siRNA oligomer bearing ApaI and EcoRI overhangs into the pSilencer 1.0 U6 vector. The upper and lower oligomer sequences used were 5′-GGACTATCGGGAGAAAGTGTTCAAGAGACACTTTCTCCCGATAG TCCTTTTTT-3′ and 5′-AATTAAAAAAGGACTATCGGGAGAAAGTGTC TCTTGAACACTTTCTCCCGATAGTCCGGCC-3′, respectively. These oligonucleotides were designed based on the human 14-3-3θ siRNA sequence (24). ^{35}S Promix, [γ-^{32}P]ATP and $^{32}P_i$ were obtained from NEN-Dupont. Anti-Myc antibody (9E10), phosphoserine antibody, olomoucine, LY294002, DRB, U0126, and H-89 were purchased from Calbiochem; the calnexin, phosphothreonine, phosphotyrosine, cyclin D, cyclin A, phospho-c-Jun, cyclin-dependent kinase 2 (CDK2), 14-3-3β, 14-3-3θ, 14-3-3σ, and ERK 1/2 antibodies were obtained from Santa Cruz Biotechnology. Wheat germ agglutinin, LiCl, calphostin C, and digitonin were obtained from Sigma.

Cell culture and transfection. COS-1and Huh-7 cells were maintained in Dulbecco's modified Eagle's medium supplemented with penicillin, streptomycin and 10% fetal bovine serum. Cells were transfected with Lipofectamine reagent as per the manufacturer's instructions. Mock-transfected cells were transfected with the empty vector. For synchronization experiments, 24 h postseeding, cells were starved for 34 h in serum-free medium followed by stimulation with 10% serum-containing medium for the indicated time periods.

Metabolic labeling, drug treatment, and immunoprecipitation. Forty hours posttransfection, cells were starved for 1 h in cysteine- and methionine-deficient medium, and then labeled with 100 μCi of ^{35}S Cys/Met Promix for 4 h. After labeling, cells were washed once in phosphate-buffered saline, and lysed in lysis buffer (20 mM Tris-HCl, pH 7.5; 150 mM NaCl; 1 mM EDTA; 1 mM EGTA; 1% Triton; 2.5 mM sodium pyrophosphate; 1 mM β-glycerolphosphate; 1 mM Na_3VO_4) with protease inhibitor cocktail. Fororthophosphate labeling, cells were starved for 3 h in phosphate-free medium followed by labeling with 350 μCi of ^{32}P-labeled orthophosphoric acid for 2 h. After labeling, cells were lysed as described above.

For immunoprecipitation, equal amounts of protein were incubated overnight with 1 μg of the corresponding antibody. This was followed by 1 h incubation with 100 μl of 10% protein A-Sepharose suspension. The beads were washed four times with lysis buffer, and protein was eluted by boiling the samples in 2x sodium dodecyl sulfate (SDS) dye. Proteins were then resolved in 12% SDS-polyacrylamide gel electrophoresis (PAGE). For immunodepletion, cell lysate was incubated with 2 μg of ERK1/2 antibody overnight followed by incubation with 100 μl 10% suspension of protein A-Sepharose for 1 h. The supernatant was then incubated with 1 μg of ERK1/2 antibody and processed along with other samples for immunoprecipitation as described above. Data obtained are representative of three independent sets of experiments conducted. Results were quantified and normalized values were calculated using the NIH Image V:1.32 program. The graphs represent ± standard error of the mean of three independent sets of experiments.

All the inhibitors were added at a permissible concentration (depending on their 50% inhibitory concentration value) as reported earlier. All inhibitors except DRB (5,6-dichlorobenzimidazole 1-β-D-ribofuranoside) was added during the starvation period and maintained throughout the labeling period. DRB was added 13 h prior to starvation and maintained during labeling. The final concentration of different inhibitors was H89, 50 nM; LY294002, 10 μM; U0126, 10 μM; olomoucine, 15 μM; lithium chloride, 10 mM; calphostin C, 50 nM; U0126, 10 nM; DRB, 30 μM. These concentrations have earlier been reported to be noncytotoxic for the host (3, 7, 10, 21–23).

Nuclear import was blocked using wheat germ agglutinin as described earlier with minor modifications (4). Briefly, cells were maintained in phosphate-free medium for 3 h and then permeabilized in digitonin (25 μg/ml) for 3 min at 4°C in the presence of an ATP regenerating system (5 mM ATP, 5 mM creatine phosphate and 20U/ml creatine phosphokinase). These cells were then incubated with wheat germ agglutinin (20 μg/ml) for 5 min followed by 30 min labeling with 350 μCi [^{32}P]orthophosphate at 37°C. The nuclear and cytosolic fractions were separated and immunoprecipitated using anti-Myc antibody. Western blotting was done as described earlier (18). Protein bands were detected by enhanced chemiluminescence method using a commercially available ECL kit (Cell Signaling Technology, USA) following the manufacturer's protocol.

Immunofluorescence assay. Immunofluorescence staining was done as described previously (18).

Nuclear fractionation. Cells were washed once in phosphate-buffered saline and resuspended in 400 μl of ice-cold buffer A (10 mM HEPES, pH 7.9, 0.1 mM EDTA, 0.1 mM EGTA, 1 mM dithiothreitol, protease inhibitor cocktail) by gentle pipetting and kept on ice for 15 min followed by addition of 25 μl of 10% NP-40 and vigorous vortexing for 10 seconds. Subsequently, the samples were spun for 30 seconds in a microfuge and the supernatant was used as cytoplasmic fraction. The pellet was washed again with buffer A and used as the nuclear fraction. Both the fractions were used for immunoprecipitation as described above.

TABLE 1. Putative phosphorylation sites for the N protein of SARS-CoV

Enzyme	Recognition sequence[a]	Predicted position[b]	Pattern[c]
CDK	*RGNSPAR*	*204–210*	*. . .([ST])P.[KR]*
CK2	*TGPE*	*116–119*	*([ST]). .E*
	SAAE	*251–254*	
GSK3	SNQRS	8–12	([ST]). . .S
	SRGGS	177–181	
	SQASS	181–185	
	SSRSS	184–188	
	SRSSS	185–189	
	SSSRS	187–191	
	SRGNS	191–195	
	STPGS	198–202	
	TPGSS	199–203	
	SRGNS	203–207	
PKA	RIT	15–17	R.([ST])
	RAT	90–92	
	RSS	186–188	
	RNS	196–198	
PKB	RSRGNSR	190–196	R.R. .([ST]).
PLK	EASL	119–122	[DE].[ST][ILFWMVA]
CK1	SWFT	52–55	S. .([ST])
	SQAS	181–184	
	SSRS	184–187	
	SRSS	185–188	
	SSRS	188–191	
	SRNS	195–198	
	SKVS	233–236	
MAPK	AEVSPRW	103–109	. . .([ST])P. .
	ALNTPKD	139–145	
	RNSTPGS	196–202	
	MEVTPSG	323–329	

[a] Respective amino acid sequence of N protein responsible for recognition by the corresponding enzyme.
[b] Number of amino acids from the N terminus.
[c] Putative consensus amino acid sequence required for recognition by the respective enzyme. [ ], either/or substitution; ( ), possible presence of both amino acid residues.

Membrane fractionation. Membrane fractionation was done as described by Wiertz et al. (25) with minor modification. Briefly, cells were washed once in phosphate-buffered saline and resuspended in isotonic buffer (250 mM sucrose, 10 mM triethanolamine, 10 mM acetic acid, 1 mM EDTA, pH 7.4, and protease inhibitor cocktail). Further, the cells were homogenized by passing 10 times in a 25-gauge needle followed by six passages through a 27-gauge needle. Samples were then centrifuged twice at 1,000 × g for 10 min at 4°C and clarified lysate was again centrifuged at 1,00,000 × g for 90 min at 4°C in an ultracentrifuge (Beckman). The supernatant was used as the cytoplasmic fraction and the pellet was used as the total membrane fraction. Immunoprecipitation was conducted as described above.

Protein expression by coupled in vitro transcription-translation. pCDNA3.1 or pCDNA3.1 N plasmid was used for in vitro N protein expression. Transcription in this case was initiated from the T7 promoter and the resultant transcript was translated by the translation machinery present in the rabbit reticulocyte lysate. The reaction was assembled using a commercially available TNT kit (Promega Corp., USA) following the manufacturer's protocol. The resultant protein was stored at −20°C. An aliquot of the lysate was mixed with equivalent amounts of 2× SDS loading dye and boiled for 5 min and the protein bands were visualized by SDS-PAGE followed by staining in Coomassie brilliant blue.

In vitro phosphorylation assay. Immunoprecipitated cell lysates were washed twice with kinase buffer (25 mM Tris, pH 7.5, 5 mM β glycerolphosphate, 2 mM dithiothreitol, 0.1 mM Na_3VO_4, 10 mM $MgCl_2$) and then incubated with 10 μg of in vitro translated protein or 1 μg each of histone H1 or maltose-binding protein, respectively, 100 μM ATP and 10 μCi of [γ-^{32}P]ATP for 45 min at 30°C.

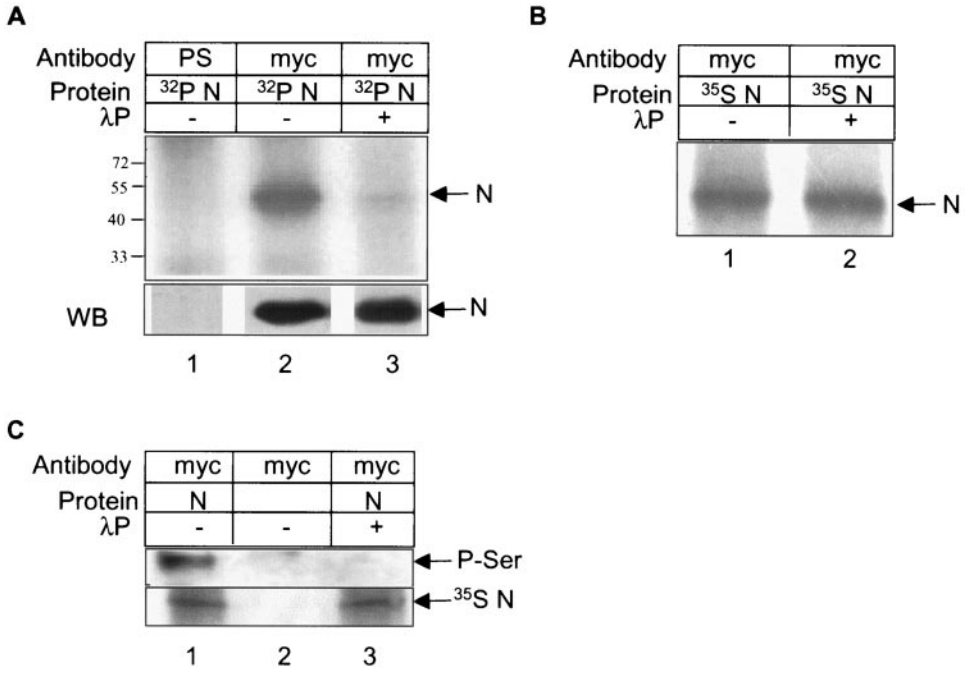

FIG. 1. N protein is phosphorylated. (A) pCDNA3.1 N Myc-transfected and [^{32}P]orthophosphate-labeled cell lysates were immunoprecipitated with preimmune serum (lane 1) or with anti-Myc antibody (lanes 2 and 3). Equal amounts of immunoprecipitated samples were treated with 400 units of λ phosphatase (lane 3). Samples were resolved in 12% SDS-PAGE and bands were detected by autoradiography. In the lower panel, 25% of each lysate was immunoprecipitated and Western blotted with anti-Myc antibody and the signal was detected by the enhanced chemiluminescence method. (B) pCDNA3.1 N Myc-transfected and ^{35}S Promix-labeled cell lysates were untreated (lane 1) or treated with 400 units of λ phosphatase (lane2) and immunoprecipitated using anti-Myc antibody. Bands were detected by autoradiography. (C) pCDNA3.1 (lane 2) or pCDNA3.1 N (lanes 1 and 3)-transfected and ^{35}S Promix-labeled cells were immunoprecipitated with anti-Myc antibody and Western blotted with phosphoserine antibody. Equal amounts of immunoprecipitated lysates were treated with 400 units of λ phosphatase (lane 3). The same blot was air dried and exposed to X-ray film overnight to check the level of N expression (lower panel).

Histone H1 or maltose-binding protein samples were used directly after boiling for 5 min in 10 μl 4X SDS dye. Samples containing N protein were again immunoprecipitated using anti-Myc antibody, and proteins eluted by boiling in 2X SDS dye. Protein bands were resolved by 12% SDS-PAGE and detected by autoradiography.

RNA isolation, cDNA subtraction, and Northern analysis. RNA was isolated from transfected COS-1 cells using RNeasy kit (QIAGEN) as described by the manufacturer. cDNA subtraction was conducted as described in Singh et al. (17). Northern analysis was performed as described by Sambrook et al. (16).

RESULTS AND DISCUSSION

The nucleocapsid protein of SARS virus is a predicted phosphoprotein of 46 kDa. In silico analysis using the NET PHOS 2.0 program revealed multiple putative phosphorylation sites for glycogen synthase kinase, protein kinase A, casein kinase I, casein kinase II, and one site each for cyclin-dependent kinases (CDK), protein kinase B, mitogen-activated protein kinase, and Polo-like kinase (Table 1). This analysis indicates that the N protein gets phosphorylated at multiple residues.

Based on these predictions, we conducted initial experiments to test if N undergoes phosphorylation in vivo. Plasmids expressing C-terminally Myc-tagged N (pCDNA 3.1 Myc N) were transfected into COS-1 cells as described in Materials and Methods; 40 h posttransfection, cells were labeled with 350 μCi of [^{32}P]orthophosphoric acid for 2 h, and immunoprecipitated using anti-Myc antibody. The immunoprecipitated proteins were resolved in 12% SDS-PAGE and detected by autoradiography. As shown in Fig. 1A, mock-immunoprecipitated (using preimmune serum) cells did not show any phosphate-labeled protein (Fig. 1A, lane 1) whereas N immunoprecipitated (using anti-Myc antibody) cells showed the N protein migrating at ~48 kDa (Fig. 1A, lane 2), which corresponds to the approximate molecular size of the protein.

In order to prove that the observed band corresponds to the phosphorylated N protein, aliquots of the sample were treated with λ phosphatase, which resulted in significant decrease of the corresponding phosphoprotein band (Fig. 1A, lane 3). As a control to this experiment, simultaneously we expressed ^{35}S Promix-labeled N protein (Fig. 1B, lane 1) and treated it with λ phosphatase (Fig. 1B, lane 2), to find that there was no decrease in band intensity, thus indicating that the enzyme was specifically removing only the phosphate residues from the protein. These experiments thus proved that the largely reduced band intensity in ^{32}P-labeled N was not due to contaminating protease activity in λ phosphatase, but instead due to the removal of phosphate from the protein. In order to show that the N protein was present in equal amounts in all samples, aliquots of the lysate were Western blotted using anti-Myc antibody (Fig. 1A, lower panel). Similar results were obtained when the N protein was expressed in SARS-CoV permissive (9) human hepatoma (Huh-7) cells (data not shown).

Subsequently, experiments were designed to investigate whether serine, threonine, or tyrosine or a combination of these were involved in the nucleocapsid protein phosphorylation. This was done by immunoprecipitating N-expressing cell

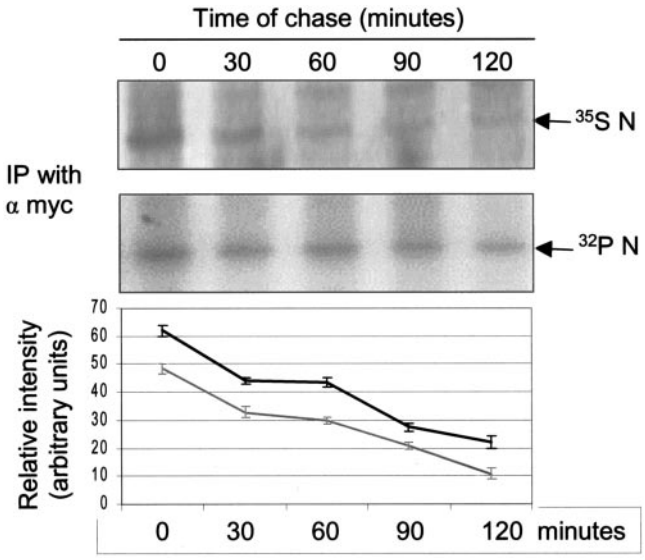

FIG. 2. Pulse-chase analysis of N protein. pCDNA3.1 N-transfected cells were labeled with ^{35}S Promix (upper panel) or [^{32}P]orthophosphate (lower panel), chased in complete medium for the indicated time periods, and the N protein was immunoprecipitated using anti-Myc antibody. Protein bands were detected by autoradiography. The figure shows a representative gel from one of three sets of experiments. The graph shows the average ± standard deviation of three independent sets of experiments. The gray line represents the total N protein. The black line represents phosphorylated N protein. The *x* axis represents time and the *y* axis represents relative band intensity at different time points.

lysates with anti-Myc antibody and then Western blotting the samples with a phosphorylation-specific antibody. As shown in Fig. 1C, only the phosphoserine-specific antibody could detect the N protein. We were unable to detect any band corresponding to N using phosphothreonine and phosphotyrosine antibodies (data not shown). However, the possibility of low-level phosphorylation at these residues cannot be ruled out owing to limited sensitivity of the immunoblotting procedure.

In order to discriminate against possible cross-reactivity of the anti-Myc antibody and phosphorylation-specific antibodies, the cells had been labeled with ^{35}S Promix and the same Western blot was air dried and exposed to X-ray film to detect the expression of N (Fig. 1C, lower panel). To show that phosphoserine antibody recognized phosphorylated residues only, aliquots of the sample were treated with λ phosphatase prior to immunoprecipitating with anti-Myc antibody (Fig. 1C, lane 3). The corresponding band in this control experiment was undetectable. Hence we conclude from these experiments that the majority of N protein is serine-phosphorylated.

Further, we checked the kinetics of the N protein phosphorylation by performing a pulse-chase assay of the protein labeled with [^{32}P]orthophosphate and compared this with the corresponding levels of ^{35}S Promix-labeled N protein. COS-1 cells were pulse-labeled for 20 min with 500μCi of [^{32}P]orthophosphate or 250 μCi of ^{35}S Promix, respectively, and then chased in complete medium for 30, 60, 90, or 120 min. Equal amounts of the protein were immunoprecipitated using anti-Myc antibody (Fig. 2). The lower panel shows that N was phosphorylated stably throughout the chase period in comparison to the total protein labeled with ^{35}S Promix (upper panel). The graph shows relative band intensity of the phosphorylated and total N protein at different time points as derived from three independent sets of experiments. The data suggest that the N protein is phosphorylated immediately after synthesis and remains stably phosphorylated.

We further investigated whether phosphorylation regulated the spatial distribution of the N protein within the cell. The functional activity of many cellular proteins is known to be regulated by altered spatial distribution following posttranslational modification, e.g., many cell cycle regulatory proteins such as p27 and CDC6 are regulated by this mechanism (13). Nucleocapsid proteins in other coronaviruses have been shown to be distributed in both the nucleus and cytoplasm (26). In order to find out whether the N protein of SARS localizes in the nucleus, nuclear and cytoplasmic fractions were isolated from ^{35}S Promix-labeled N-transfected COS-1 cells and immunoprecipitated using anti-Myc antibody. Surprisingly, N was found to be abundantly present in the cytoplasmic fraction (Fig. 3A, upper panel). Very little N protein was found in the nuclear fraction (lane 4).

To rule out any possibility of cross contamination between the cytoplasmic and nuclear fractions, an aliquot of the lysate was Western blotted with anticalnexin antibody. Calnexin is known to localize in the cytoplasm and membrane. In this experiment, we detected a band only in the cytoplasmic fraction (Fig. 3B, upper panel) indicating that there is no cross contamination between nuclear and cytoplasmic fractions. To rule out the possibility of nuclear contamination of the cytoplasmic fraction, an aliquot of the lysate was Western blotted with phospho-c-Jun antibody, which showed exclusive nuclear distribution (Fig. 3B, lower panel).

The cellular localization pattern of the N protein was further verified by an indirect immunofluorescence assay using anti-Myc antibody, whereby the N protein was found to be in the cytoplasm (Fig. 3C, left panel images). Cells were stained with DAPI (blue color) which stains the nucleus and N protein was stained with Texas red (red color). In Fig. 3C, right panel images show superimposition of nuclear stain over the Texas red stain in the same field to show any possible colocalization. Similar distribution pattern was also observed when N protein was checked for colocalization with 14-3-3 (Fig. 6C, discussed later). We then performed a nuclear fractionation assay using [^{32}P]orthophosphate-labeled N-expressing cells to check the distribution of the phosphorylated N protein. Although we could detect significant amounts of N in the cytoplasmic fraction (Fig. 3A, lower panel, lane 2), we were unable to detect any in the nuclear fraction (Fig. 3A, lane 4).

The immunofluorescence assay showed a prominent staining of the N protein around the plasma membrane. Hence we checked by biochemical fractionation whether the N protein associated with cell membrane. Immunoprecipitation of the membrane fraction with anti-Myc antibody revealed association of a significant amount of the N protein with the membrane (Fig. 3D, upper panel). Similarly, phosphorylated N was also found to associate with the membrane (Fig. 3D, lower panel).

Having seen phospho-N localization predominantly in the cytosolic fraction, we further investigated whether the N protein was phosphorylated in the cytosol or whether N gets phos-

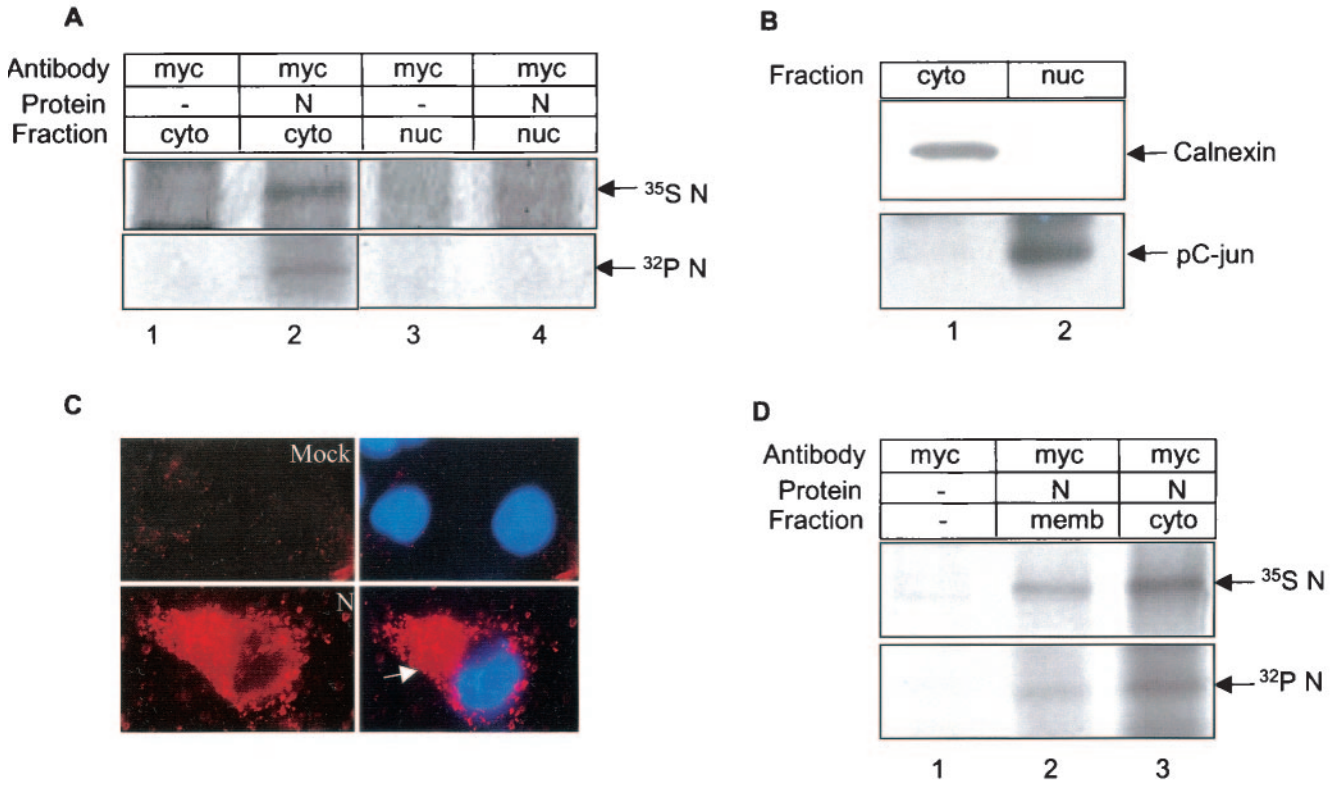

FIG. 3. Subcellular localization of N protein. (A) pCDNA 3.1 (lane 1 and 3) or pCDNA3.1 N (lane 2 and 4)-transfected cells labeled with [^{32}P]orthophosphate (lower panel) or ^{35}S Promix (upper panel) were fractionated and immunoprecipitated using anti-Myc antibody. Lanes 1 and 2: cytoplasmic fraction; lanes 3 and 4: nuclear fraction. (B) Cytoplasmic (lane 1) and nuclear (lane 2) fractions from control cell lysates were Western blotted with anti-calnexin (upper panel) and phospho-c-Jun (lower panel) antibody. (C) Mock (upper panel) or pCDNA 3.1 N (lower panel)-transfected cells were probed with anti-Myc antibody followed by Texas red and DAPI staining and the corresponding fluorescence was visualized using an immunofluorescence microscope. The left panel shows image of N expression and right panel shows a merged image of nuclear staining (DAPI) over the Texas red stain in the same field. The arrow shows cytoplasmic localization of the N protein. (D) pCDNA 3.1 (lane 1) or pCDNA 3.1 N (lanes 2 and 3)-transfected cells were labeled with ^{35}S Promix (upper panel) or [^{32}P]orthophosphate (lower panel). The membrane (lane2) and cytoplasmic (lane 3) fractions were immunoprecipitated with anti-Myc antibody. Radiolabeled proteins were detected by autoradiography.

phorylated in the nucleus and subsequently exported into the cytoplasm. In order to check this hypothesis, we blocked nuclear protein import using wheat germ agglutinin and observed the phosphorylation of N. N protein was found to be effectively phosphorylated despite the presence of the inhibitor, indicating that a cytosolic kinase was responsible for phosphorylation of the N protein (Fig. 4A). However, the possibility exists that multiple kinases phosphorylate N both in the cytoplasm and nucleus.

Among the putative kinases predicted to phosphorylate N (Table 1), the cyclin-CDK complex is known to be active inside the nucleus (13) and some others can act in both the nucleus and cytoplasm. Hence the possibility of the N protein's getting phosphorylated both in the cytoplasm and the nucleus seemed possible. In order to check this, we used a series of inhibitors that were specific for different enzymes and examined their ability to block the phosphorylation of N. As shown in Fig. 4B, some of the inhibitors were able to inhibit the phosphorylation of N significantly however none of the inhibitors could singly block phosphorylation completely, which is in agreement with our in silico analysis.

Interestingly, a combination of inhibitors effectively blocked phosphorylation almost completely (Fig. 4B, lane 2), thus implying that in vivo N is phosphorylated at multiple sites by multiple kinases. Moreover, the data also reveal that not all putative phosphorylation sites are functional in vivo, since the phosphatidylinositol 3-kinase inhibitor LY294002 as well as the protein kinase A inhibitor (H89) were unable to show any significant inhibition of N protein phosphorylation. However, this might not be true during a natural viral infection if other viral proteins were engaged in modulating the cellular as well as viral protein networks causing these sites to get preferentially phosphorylated.

Besides LiCl (glycogen synthase kinase 3 inhibitor), U0126 (mitogen-activated protein kinase inhibitor), and DRB (casein kinase II inhibitor), an inhibitor that could block N protein phosphorylation to a lesser extent but significantly (~30% inhibition) was olomoucine, which is known to inhibit cyclin-dependent kinase activity by acting as a competitive inhibitor for the ATP binding domain of the enzyme (11). CDKs are active as enzymes only when bound to their respective cyclins and the turnover of cyclins is strictly regulated in a cell cycle-dependent manner (13). Hence, N protein might be modulating the activity of cellular substrates of the cyclin-CDK complex by binding to and getting phosphorylated by the latter.

To investigate if the N protein is a direct substrate of the

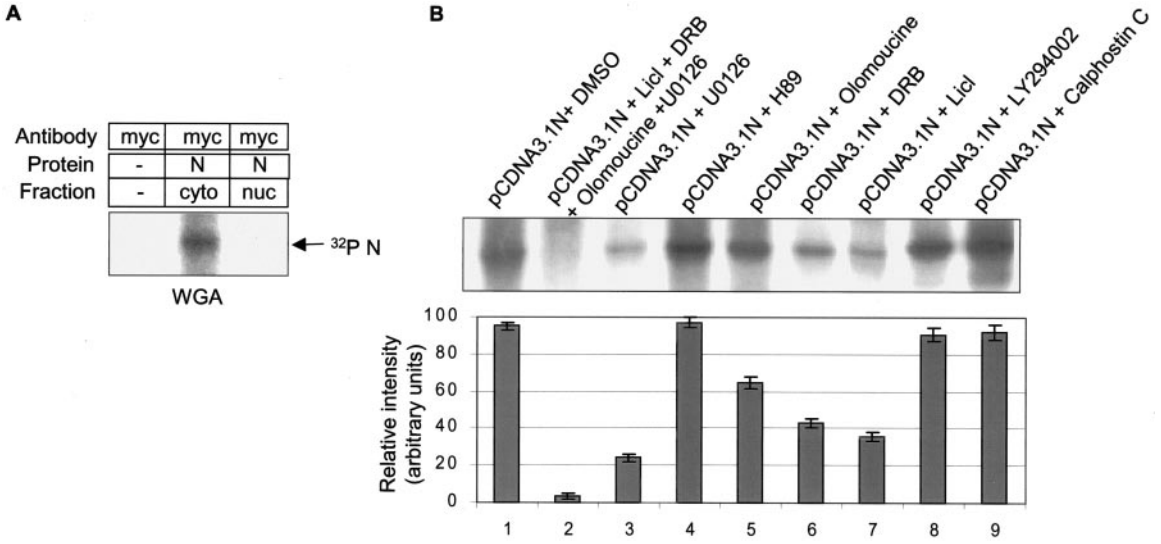

FIG. 4. Effect of different inhibitors on N phosphorylation. (A) pCDNA3.1 N-transfected cells were treated with wheat germ agglutinin (20 μg/ml) during the starvation and labeling period. Cytoplasmic (lane 2) and nuclear (lane 3) fractions were immunoprecipitated using anti-Myc antibody, resolved by 12% SDS-PAGE, and the protein bands were detected by fluorography. Lane 1 represents pCDNA3.1-transfected cells treated with wheat germ agglutinin (WGA) whole-cell extract processed simultaneously. (B) pCDNA3.1 N-transfected cells were treated with different inhibitors, labeled with [^{32}P]orthophosphate, and the samples were subsequently immunoprecipitated using anti-Myc antibody. The upper panel shows a representative gel. The band intensities were quantified from three independent sets of experiments and the average relative intensity ± standard deviation was calculated as shown in the bar graph.

cyclin-CDK complex, we analyzed the ability of the cyclin-CDK complex to phosphorylate in vitro-expressed N by performing an in vitro phosphorylation assay. The N protein was expressed using a rabbit reticulocyte lysate-based coupled transcription-translation system (TNT kit, Promega, USA) and expression of the N protein was verified on 12% SDS-PAGE from a small fraction of the reaction and staining by Coomassie brilliant blue (Fig. 5A). In order to immunoprecipitate cyclins D and A during their maximum endogenous levels, COS-1 cells were synchronized at the G_0 phase of the cell cycle by serum starvation for 34 h and then stimulated with 10% serum to initiate cell cycle progression. Cells were harvested at 2, 12, 18, and 22 h poststimulation and aliquots of the lysate were Western blotted with cyclin D and cyclin A, whose expression begins during the G_1 and S phases, respectively.

As shown in Fig. 5B, upper panel, cyclin D was detected at all time points, whereas cyclin A was maximally detected at 18 and 22 h (Fig. 5B, middle panel). As a control to check equal loading of protein, the cyclin D blot was stripped and reprobed with antibody to CDK2, which is present during all phases of cell cycle (Fig. 5B, lower panel). Based on these observations, cells were harvested at 2 and 18 h poststimulation, immunoprecipitated using cyclin A or cyclin D antibody, and used in the in vitro phosphorylation assay as described in Materials and Methods. As shown in Fig. 5C, immunoprecipitated cyclin A and cyclin D could effectively phosphorylate the N protein, where as no corresponding band was observed in mock-translated or preimmune serum-immunoprecipitated samples. Further, the band intensity was found to be significantly reduced when treated with λ phosphatase (Fig. 5C, lanes 5 and 10, N+λ). This confirmed that the N protein was indeed a substrate of the cyclin-CDK complex. Histone H1, which is a well-known substrate of the cyclin-CDK complex, was used as a positive control for this experiment (Fig. 5C, lane 11).

Similarly, we performed the in vitro phosphorylation assay of N protein to check whether it is a substrate of mitogen-activated protein kinase. For this, cells were seeded in 60-mm dish at 50% confluence and 48 h postseeding cells were immunoprecipitated using anti-ERK1/2 antibody and in vitro phosphorylation was done as described above. As shown in Fig. 5D, N was found to be a substrate of the mitogen-activated protein kinases ERK1 and 2 (Fig. 5C, lane 2). Mock-translated, λ phosphatase-treated, and preimmune serum samples were used as controls. Also an aliquot of the sample was immunodepleted of ERK1/2 and processed simultaneously for in vitro phosphorylation to show the specificity of enzyme (Fig. 5C, lane 3). Maltose-binding protein was used as a positive control substrate to check the mitogen-activated protein kinase activity (Fig. 5C, lane 6).

In order to prove the hypothesis that the N protein is phosphorylated in the nucleus and then translocated to the cytoplasm, we performed a nuclear fractionation assay of ^{35}S-labeled N-expressing cells in the presence of different phosphorylation inhibitors and looked for the presence of N protein in the nuclear fraction. As expected, in the presence of olomoucine, a significant fraction of the N protein was found to localize in the nuclear fraction. Further, DRB-treated cells also showed a fraction of N protein in the nucleus. In contrast, LiCl- and U012-treated cells showed the majority of the protein in the cytoplasmic fraction, indicating that either glycogen synthase kinase 3 and mitogen-activated protein kinase phosphorylation is dispensable for nucleocytoplasmic shuttling of the N protein or essential for nuclear translocation and/or CDK and casein kinase II-mediated phosphorylation of the N

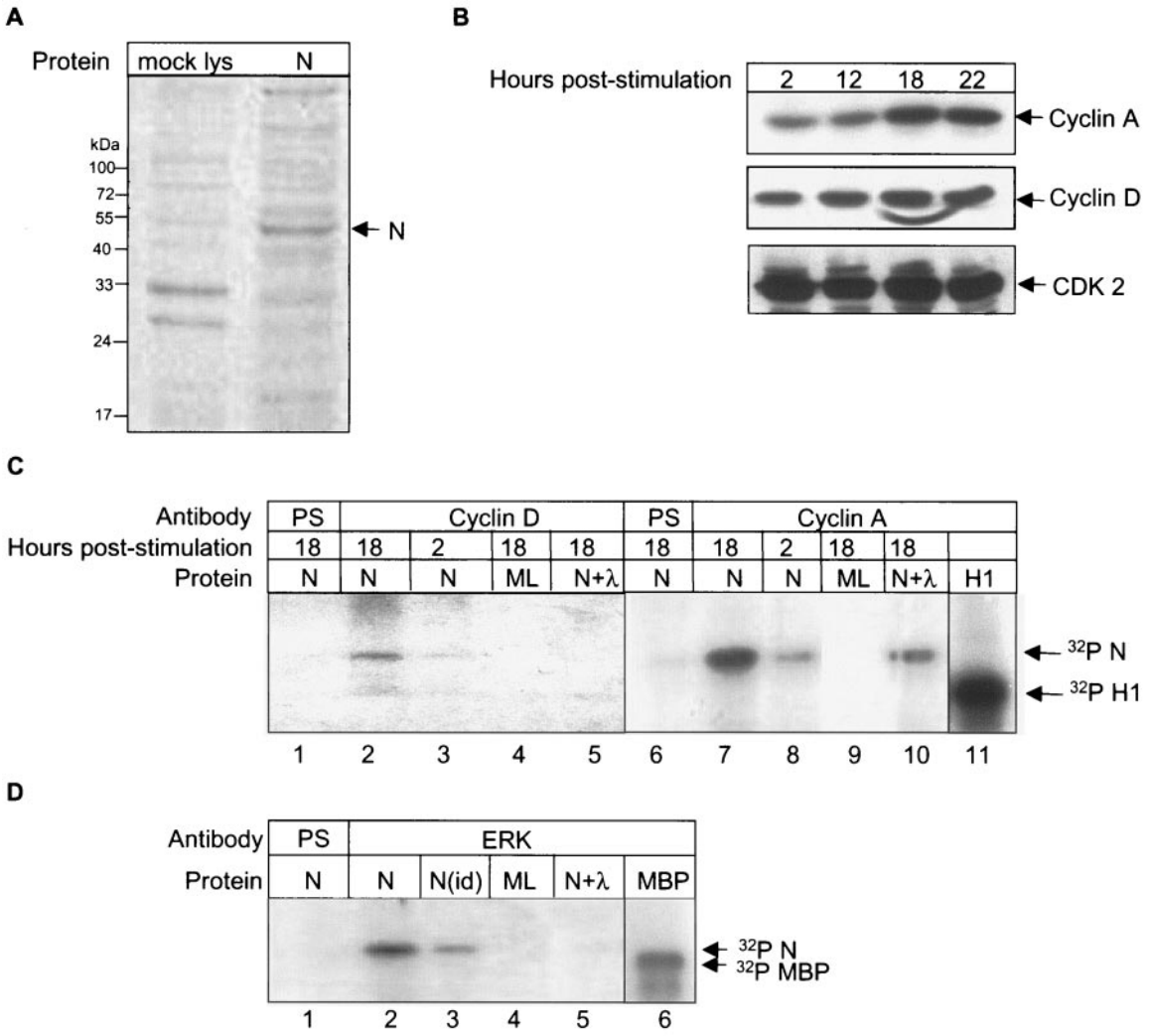

FIG. 5. In vitro phosphorylation of the N protein by cyclin-CDK complex and mitogen-activated protein kinase. (A) Coomassie brilliant blue-stained gel showing expression of the N protein (lane 2) in an in vitro translation reaction. Lane 1 represents mock-translated lysate. (B) COS-1 cells were starved for 34 h in serum-free medium, stimulated with complete medium for the indicated times, and equal amounts of the lysates were Western blotted using cyclin A (upper panel), cyclin D (middle panel), and CDK2 (lower panel) antibodies. Bands were detected by the enhanced chemiluminescence method. (C) COS-1 cells were starved for 34 h in serum-free medium, stimulated with complete medium for the indicated periods, and immunoprecipitated using the respective antibodies followed by incubation with in vitro-expressed N protein (lanes 1, 2, 3, 5, 6, 7, 8, and 10) or mock-expressed lysate (ML; lanes 4 and 9). Lanes 1 and 6 were immunoprecipitated using preimmune serum (PS). Bands corresponding to in vitro-phosphorylated N were observed by autoradiography. Lanes 5 and 10 represents N protein treated with λ phosphatase. Lane 11 shows phosphorylated histone H1. Lane 11 is a gel exposed for a shorter period. (D) In vitro phosphorylation of N protein by ERK1/2. COS-1 cells were immunoprecipitated using preimmune serum (lane 1) or ERK1/2 antibody (lanes 2 to 5). Lane 3 represents ERK1/2 immunodepleted sample. Lanes 4 and 5 represent mock lysate (ML) and λ phosphatase-treated samples, respectively. Lane 6 shows the phosphorylated maltose-binding protein band. Lane 6 was exposed for a shorter period.

protein. Interestingly, cells treated with all four inhibitors together showed that most of the N protein was localized in the cytoplasmic fraction, which further supported the above hypothesis (Fig. 6A).

Since phosphorylated N protein localized exclusively in the cytoplasm, we reasoned that phosphorylated N protein was immediately translocated to the cytoplasm. Amino acid sequence analysis of N protein revealed a putative 14-3-3 binding motif between 186 and 191 amino acid residues from the N terminus. 14-3-3 proteins are known to bind serine/threonine-phosphorylated ligands and transport them to the cytoplasm (14) besides taking part in many other cellular activities (8, 20). Hence, we checked the ability of N protein to bind 14-3-3.

Mock-transfected or N-transfected cells were immunoprecipitated using the respective antibodies and Western blotted using 14-3-3 β antibody that recognizes all the 14-3-3 isoforms (Fig. 6B, upper panel). N protein was found to coimmunoprecipitate with 14-3-3 (Fig. 6B, lane 3). Since 14-3-3 is known to interact with the cargo in a phosphorylation-dependent manner, and we had earlier seen that a cocktail of inhibitors could almost block the phosphorylation of N protein, we simultaneously coimmunoprecipitated N protein maintained with the

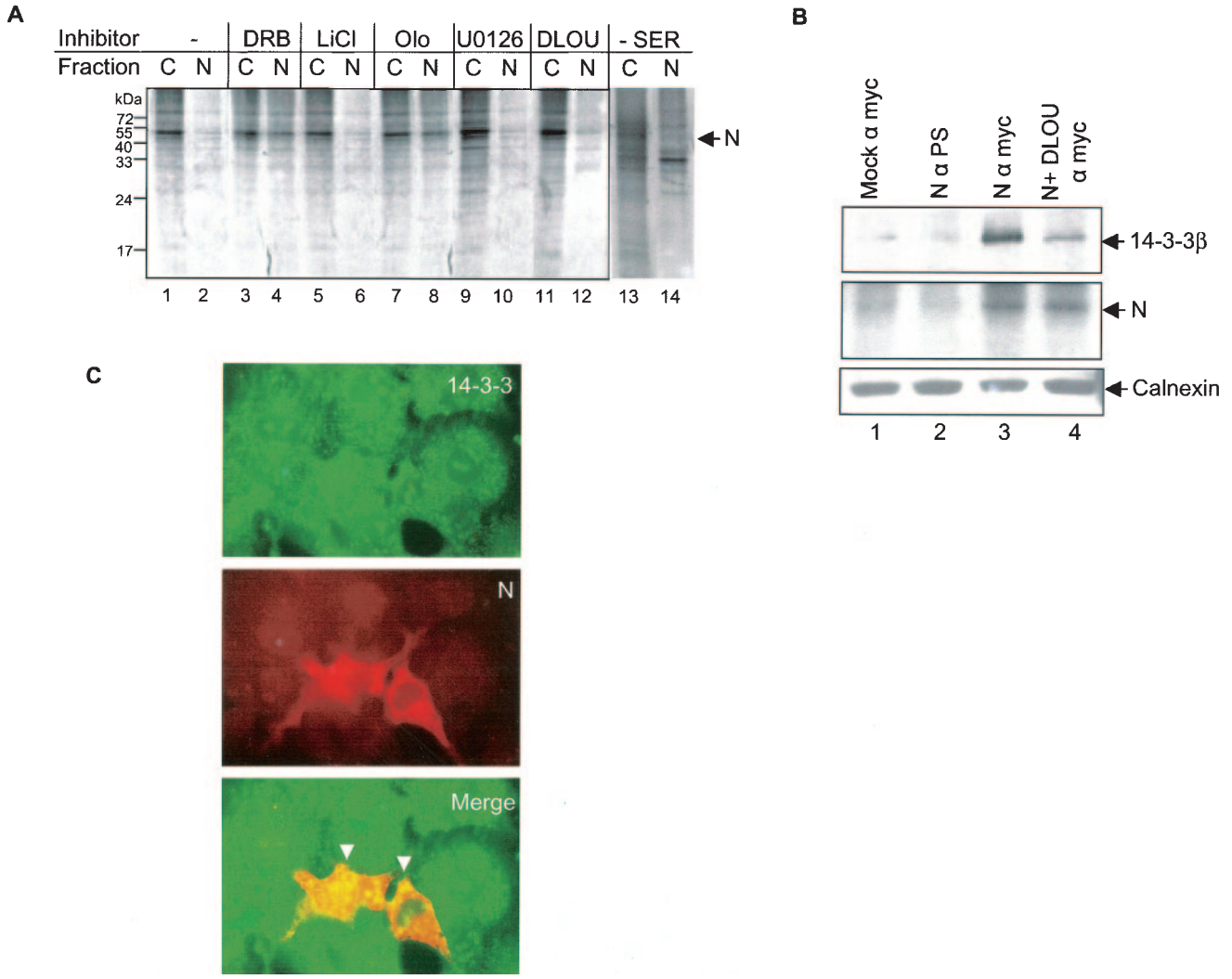

FIG. 6. Phosphorylation-dependent 14-3-3 binding translocates N protein to the cytoplasm. (A) COS-1 cells transfected with pCDNA3.1 N were treated with carrier only or with inhibitors or cells were serum starved for 24 h (lanes 13 and 14); labeled with ^{35}S Promix, and cytoplasmic(C) and nuclear (N) fractions were immunoprecipitated using anti-Myc antibody, resolved by 12% SDS-PAGE, and bands were detected by fluorography. O, olomoucine; U, U0126; D, DRB; L, LiCl. (B) pCDNA 3.1 (mock; lane1) or pCDNA 3.1 N (lane 2, 3 and 4)-transfected cells labeled with ^{35}S Promix were immunoprecipitated using the indicated antibodies (i.e., preimmune serum for lane 2 and anti-Myc antibody for lanes 3 and 4), resolved on 12% SDS-PAGE, and Western blotted using anti-14-3-3 antibody (upper panel). The same blot was air-dried and exposed to X-ray film to check the expression of N protein (middle panel) by autoradiography. A 20% aliquot of the lysate was loaded on SDS-PAGE gels, Western blotted, transferred, and probed using anticalnexin antibody (lower panel). D, DRB inhibitor was added to the lane 4 sample as described in Materials and Methods. PS, preimmune serum. (C) pCDNA3.1 N-transfected cells were stained with fluorescein isothiocyanate-labeled anti-rabbit (14-3-3 staining, upper panel) and Texas red-labeled anti-mouse (Myc-tagged N, middle panel) antibodies and fluorescence was visualized by using an immunofluorescence microscope. The lower panel shows a merged image of the upper and middle panels done by using the Adobe Photoshop 6.0 program. The arrows show colocalization between N and 14-3-3 protein.

kinase inhibitor cocktail and checked for its ability to bind to 14-3-3.

As shown in Fig. 6B, lane 4, 14-3-3 binding was significantly reduced in the presence of inhibitors. As a control to check N expression in the above samples, the same had been labeled with ^{35}S Promix, hence the blot was air dried and exposed to X-ray film (Fig. 6B, middle panel). To ensure equal loading of the samples, an aliquot of the samples was Western blotted with anti-calnexin antibody (Fig. 6B, lower panel). Similarly, the N protein was found to associate with 14-3-3 in human hepatoma cells to show that the same was true in a SARS-CoV replication competent cell line (data not shown). Further, we conducted immunofluorescence studies to colocalize N protein with 14-3-3. As shown in Fig. 6C, upper panel, 14-3-3 staining (fluorescein isothiocyanate labeled), the middle panel shows Myc-tagged N staining (Texas red labeled), and the lower panel shows a superimposition of upper panel over the middle panel. The N protein was found to colocalize with 14-3-3 in the cytoplasm (Fig. 6C, lower panel). Hence, we suggest that phosphorylated N protein associates with 14-3-3 and gets translocated to the cytoplasm.

Earlier studies in our laboratory have shown that the N

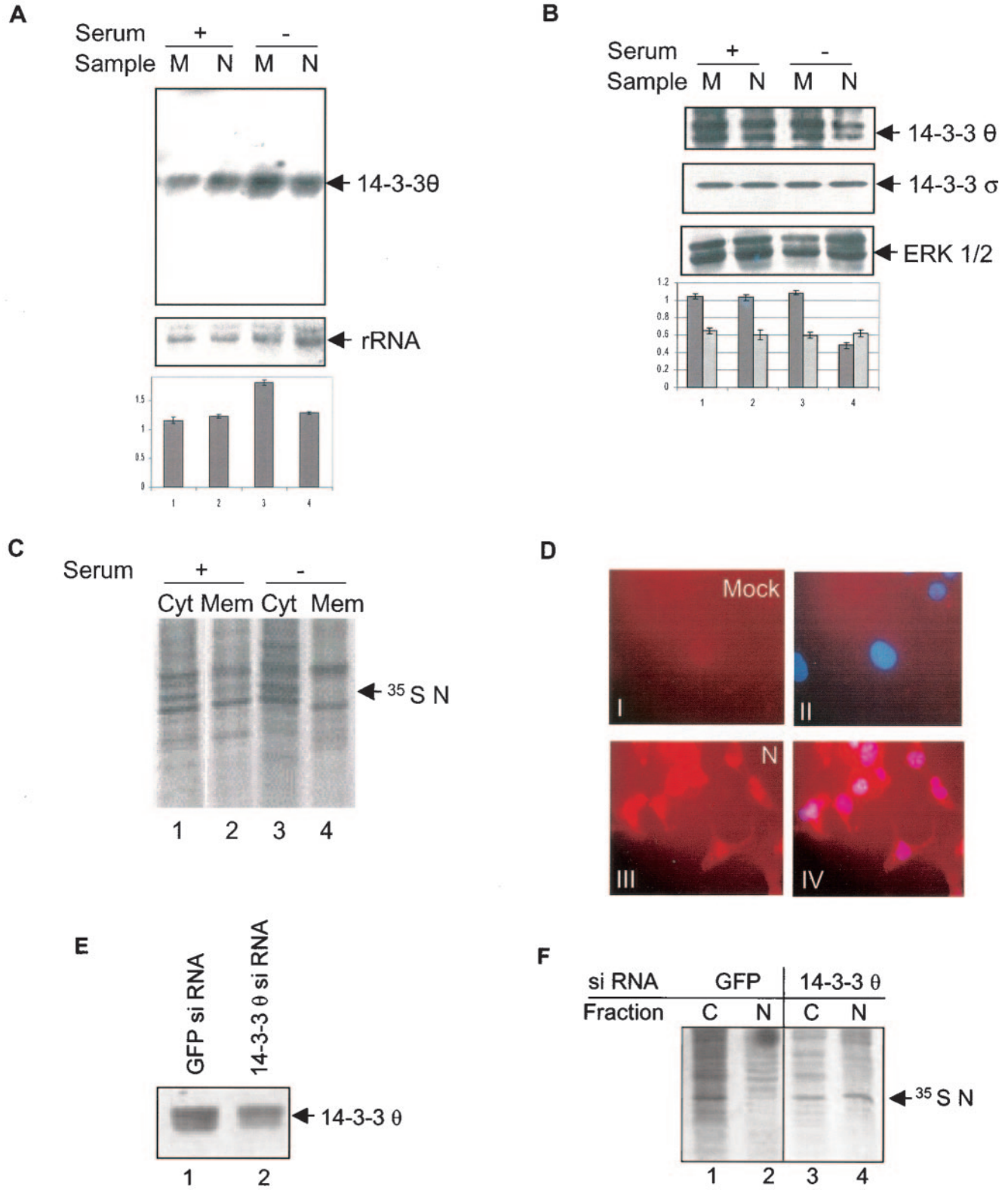

FIG. 7. N protein down-regulates 14-3-3θ expression and localizes to the nucleus in the absence of growth factors. (A) pCDNA 3.1 (lane 1 and 3) or pCDNA 3.1 N (lane 2 and 4)-transfected cells were maintained for 24 h in the indicated medium 24 h posttransfection and RNA was isolated; 15 μg of total RNA of each sample was used for Northern blotting. The upper panel shows the level of 14-3-3θ. The same blot was probed for the level of rRNA to check equal loading in each lane (lower panel). Quantification was done using NIH Image Program and band intensity was normalized with reference to rRNA, relative fold intensity was calculated and the graph was plotted. Data represent the mean of three independent experiments. (B) pCDNA 3.1 (lane 1 and 3) or pCDNA 3.1 N (lane 2 and 4)-transfected cells were maintained for 24 h in the indicated medium 24 h posttransfection and aliquots of total cell lysates were Western blotted with 14-3-3θ (first panel) or 14-3-3σ antibody (second panel). The same

protein can induce apoptosis in the absence of growth factors. In an attempt to identify the mechanism of apoptosis induction by the N protein, we were trying to identify the genes that are down-regulated in N-expressing cells in the above conditions using a PCR-based cDNA subtraction technique (17). From this experiment we observed that the level of 2 independent 1.3-kilobase cDNA was down-regulated in the absence of growth factors in N-expressing cells. Sequencing of these two clones identified them to code for the 14-3-3θ protein. This observation was further verified by a Northern blot analysis (Fig. 7A, upper panel, lane 4). However, there was no effect on 14-3-3θ levels in N-expressing cells in the presence of serum (lane 2).

The lower panel shows the rRNA level as a loading control. We further analyzed the levels of 14-3-3θ protein and found it to be down-regulated in N-expressing cells in the absence of growth factors (Fig. 7B, first panel, lane 4). However, there was no effect on 14-3-3θ protein levels in the presence of growth factors (lane 2). Next we checked whether the N protein mediated 14-3-3 down-regulation was specific for θ isoform only. For this aliquots of the lysate were immunoblotted with the anti-14-3-3σ antibody, which specifically detects σ isoform of 14-3-3. As shown in Fig. 7B (second panel), the level of 14-3-3σ was found to be unaltered in N-expressing cells despite the presence or absence of serum. The ERK1/2 level was used as a control to check equal loading (Fig. 7B, *3rd panel*). Quantification of the relative band intensity from three different experiments showed approximately 40% inhibition of 14-3-3θ expression in serum-starved N-expressing cells compared to mock-transfected cells in the same condition.

Since N expression down-regulated 14-3-3θ protein levels in the absence of growth factors, we subsequently asked whether the N protein localized to the nucleus under such conditions. Nuclear fractionation studies using ^{35}S Promix-labeled N-expressing cell lysate in the absence of serum revealed that ~80% of the protein localized to the nucleus (Fig. 6A, lanes 13 and 14). The immunoprecipitation data were further confirmed by an indirect immunofluorescence assay of N-expressing serum-starved cells, whereby the majority of the N protein was found to be present in the nuclear fraction (Fig. 7D).

Panel I shows mock- and panel III shows N-transfected cells; both stained with Texas red. Same samples were also stained with 4′,6′-diamidino-2-phenylindole (DAPI), which is a nucleus-specific dye. Panels II and IV shows superimposition of DAPI with Texas red, thus confirming nuclear localization of N protein in serum starved cells. This observation further indicates that cytoplasmic translocation of the N protein is mediated through 14-3-3 binding. Further, membrane association of the N protein was found to be lost in the absence of growth factors (Fig. 7C, compare lane 4 with lane 2). This may be attributed to the inability of the N protein to return to the cytoplasm in the absence of serum.

Since 14-3-3 interaction appeared to be crucial for cytoplasmic translocation of N protein and the levels of 14-3-3θ were found to be specifically down-regulated by the N protein, we further examined the involvement of 14-3-3θ in N protein translocation by using an siRNA approach to silence the expression of 14-3-3θ. Transfection of an siRNA expression plasmid bearing 14-3-3θ-specific sequence into COS-1 cells was found to down-regulate 14-3-3θ protein levels by approximately 50% (Fig. 7E). The fact that the siRNA was specific for the 14-3-3θ isoform was ensured by immunoblotting aliquots of the lysate with 14-3-3σ-specific antibody, the level of which remained unaltered (data not shown).

Finally, plasmids expressing the N protein and 14-3-3θ siRNA or GFP siRNA (control siRNA) were cotransfected into COS-1 cells; 48 h posttransfection, an increased amount of N protein was found to be retained in the nuclear fraction in 14-3-3θ siRNA-treated cells (Fig. 7F, lane 4) compared to GFP siRNA-treated cells (lane 2). This further confirms that 14-3-3 protein is involved in nucleocytoplasmic translocation of the N protein. However, it might be argued that the observed phenomenon is an indirect effect of inhibition of 14-3-3θ. Since 14-3-3θ regulates nucleocytoplasmic shuttling of many cellular factors, inhibition of its expression may block the activities of many factors that might influence cytoplasmic translocation of the N protein. Thus, confirmation of a direct role of 14-3-3θ in nucleocytoplasmic shuttling of the N protein warrants further investigation.

Nucleocapsid proteins of many coronaviruses have been shown to be phosphorylated (26). However, neither the mechanism nor the functional relevance of phosphorylation is known. Here, we report that SARS-CoV nucleocapsid protein is also phosphorylated by multiple kinases. The N phosphoprotein was found to be predominantly cytoplasmic, membrane associated, and relatively stable. Further, we provided evidence that N is a substrate of the cyclin-dependent kinase, glycogen synthase kinase 3, casein kinase II, and mitogen-activated protein kinase. This agrees with our in silico data which show that the N protein does bear signature motifs for

blot was stripped and probed with total ERK antibody to check for equal loading (3rd panel). The data shown are representative of three independent sets of experiments. Band intensities were quantified using NIH Image Program and values were normalized with reference to that of loading control, fold difference was calculated and average ± standard deviation were plotted in the graph (fourth panel). The dark bar and light bar in the graph represent 14-3-3θ and 14-3-3σ, respectively. (C) At 24 h posttransfection, pCDNA 3.1 N-expressing cells were maintained for further 24 h in the indicated medium, labeled with ^{35}S Promix, cytoplasmic (cyt) and membrane (mem) fractions were immunoprecipitated using anti-Myc antibody, resolved by 12% SDS-PAGE, and bands were detected by fluorography. (D) At 24 h posttransfection, mock pCDNA 3.1 (upper panel) or pCDNA 3.1 N (lower panel)-expressing cells were maintained for a further 24 h in the absence of growth factors, stained with Texas red (N staining, left panel) and DAPI (nucleus staining) and images were visualized in an immunofluorescence microscope. Image III shows nuclear and cytoplasmic staining of N-expressing cells. Right panel IV shows DAPI-stained nucleus superimposed over Texas red-stained N to show colocalization. (E) COS-1 cells were transfected with GFP siRNA (lane 1) or 14-3-3θ siRNA (lane 2) expression plasmid and 48 h posttransfection total cell lysate was immunoprecipitated and immunoblotted with anti-14-3-3θ antibody. (F) COS-1 cells cotransfected with pCDNA3.1 N and GFP (lane 1 and 2) or 14-3-3θ (lane 3 and 4) siRNA expression plasmids were separated into nuclear (N) and cytoplasmic (C) fractions 48 h posttransfection, immunoprecipitated using anti-Myc antibody, the proteins were resolved by 10% SDS-PAGE, and the bands were visualized by fluorography.

phosphorylation by these kinases. Moreover, the above data provide clues for the fact that the phosphorylated N protein shuttles from nucleus to cytoplasm by binding to 14-3-3.

Coincidentally, while following an entirely different approach to understand the apoptosis inducing property of N, we found that the latter was able to down-regulate the levels of 14-3-3θ leading to the accumulation of phosphorylated N inside the nucleus in the absence of serum. Hence, in light of these data and our previous report (18) we postulate that nuclear localization of the N phosphoprotein may be interfering with the cellular machinery, thus leading to triggering of apoptosis. However, further experiments need to be done to dissect out the exact mechanism.

From a viral point of view, we cannot pinpoint the exact functional significance of phosphorylation of N at this time. However, N phosphorylation might be serving multiple purposes to fulfill biological processes, e.g., phosphorylation may be increasing the stability of N, it may be helping in self-association of the protein, which is an essential step for viral assembly, it may be acting as a regulatory switch for subcellular localization of the protein, or it may be strategically modulating the activity of its kinases by competitively binding to their substrate binding site, thus creating a more favorable atmosphere for viral replication. Detailed analysis of such possibilities in a model system will allow critical insights into the regulatory functions of phosphorylation of the nucleocapsid protein during the SARS virus life cycle.

ACKNOWLEDGMENTS

We thank Vijay Kumar (International Centre for Genetic Engineering and Biotechnology, India) for the GFP siRNA construct used as a control in our experiments. We are also thankful to Chetan Chitins for the immunofluorescence microscope facility and Suchi Goel for technical help.

This work was supported by internal funds from the International Centre for Genetic Engineering and Biotechnology, New Delhi, and a research grant from the Department of Biotechnology to S.K.L. Collaborative support from the Microbiology Department, National University of Singapore, is gratefully acknowledged. M.S. is a Senior Research Fellow of the CSIR, India.

REFERENCES

1. **Buttner, J.** 1977. Evaluation of the diagnostic value of laboratory investigations. J. Clin. Chem. Clin. Biochem. **15:**1–12.
2. **Centers for Disease Control SARS Investigative Team and A. T. Fleischauer.** 2003. Outbreak of severe acute respiratory syndrome –worldwide. Morb. Mortal. Wkly. Rep. **52:**226–228.
3. **Chijiwa, T., A. Mishima, M. Hagiwara, M. Sano, K. Hayashi, T. Inoue, K. Naito, T. Toshioka, and H. Hidaka.** 1990. Inhibition of forskolin-induced neurite outgrowth and protein phosphorylation by a newly synthesized selective inhibitor of cyclic AMP-dependent protein kinase, N-[2-(p-bromocinnamylamino)ethyl]-5-isoquinolinesulfonamide (H-89), of PC12D pheochromocytoma cells. J. Biol. Chem. **265:**5267–5272.
4. **Connor, M. K., R. Kotchetkov, S. Cariou, A. Resch, R. Lupetti, R. G. Beniston, F. Melchior, L. Hengst, and J. M. Slingerland.** 2003. CRM1/Ran-mediated nuclear export of p27(Kip1) involves a nuclear export signal and links p27 export and proteolysis. Mol. Biol. Cell **14:**201–213.
5. **Donnelly, C. A., A. C. Ghani, G. M. Leung, A. J. Hedley, C. Fraser, S. Riley, L. J. Abu-Raddad, L. M. Ho, T. Q. Thach, P. Chau, K. P. Chan, T. H. Lam, L. Y. Tse, T. Tsang, S. H. Liu, J. H. Kong, E. M. Lau, N. M. Ferguson, and R. M. Anderson.** 2003. Epidemiological determinants of spread of causative agent of severe acute respiratory syndrome in Hong Kong. Lancet **361:**1761–1766.
6. **Egloff, M. P., F. Ferron, V. Campanacci, S. Longhi, C. Rancurel, H. Dutartre, E. J Snijder, A. E. Gorbalenya, C. Cambillau, and B. Canard.** 2004. The severe acute respiratory syndrome-coronavirus replicative protein nsp9 is a single-stranded RNA-binding subunit unique in the RNA virus world. Proc. Natl. Acad. Sci. USA **101:**3792–3796.
7. **Favata, M. F., K. Y. Horiuchi, E. J. Manos, A. J. Daulerio, D. A. Stradley, W. S. Feeser, D. E. Van Dyk, W. J. Pitts, R. A. Earl, F. Hobbs, R. A. Copeland, R. L. Magolda, P. A. Scherle, and J. M. Trzaskos.** 1998. Identification of a novel inhibitor of mitogen-activated protein kinase kinase. J. Biol. Chem. **273:**18623–18632.
8. **Giles, N., A. Forrest, and B. Gabrielli.** 2003. 14-3-3 Acts as an intramolecular bridge to regulate cdc25B localization and activity. J. Biol. Chem. **278:**28580–28587.
9. **Gillim-Ross, L., J. Taylor, D. R. Scholl, J. Ridenour, P. S. Masters, and D. E. Wentworth.** 2004. Discovery of novel human and animal cells infected by the severe acute respiratory syndrome coronavirus by replication-specific multiplex reverse transcription-PCR. J. Clin. Microbiol. **42:**3196–3206.
10. **Gopalakrishna, R., Z. H. Chen, and U. Gundimeda.** 1992. Irreversible oxidative inactivation of protein kinase C by photosensitive inhibitor calphostin C. FEBS Lett. **314:**149–154.
11. **Jackman, M., Y. Kubota, N. den Elzen, A. Hagting, and J. Pines.** 2002. Cyclin A- and cyclin E-Cdk complexes shuttle between the nucleus and the cytoplasm. Mol. Biol. Cell **13:**1030–1045.
12. **Marra, M. A., S. J. Jones, C. R. Astell, R. A. Holt, A. Brooks-Wilson, Y. S. Butterfield, J. Khattra, J. K. Asano, S. A. Barber, S. Y. Chan, A. Cloutier, S. M. Coughlin, D. Freeman, N. Girn, O. L. Griffith, S. R. Leach, M. Mayo, H. McDonald, S. B. Montgomery, P. K. Pandoh, A. S. Petrescu, A. G. Robertson, J. E. Schein, A. Siddiqui, D. E. Smailus, J. M. Stott, G. S. Yang, F. Plummer, A. Andonov, H. Artsob, N. Bastien, K. Bernard, T. F. Booth, D. Bowness, M. Czub, M. Drebot, L. Fernando, R. Flick, M. Garbutt, M. Gray, A. Grolla, S. Jones, H. Feldmann, A. Meyers, A. Kabani, Y. Li, S. Normand, U. Stroher, G. A. Tipples, S. Tyler, R. Vogrig, D. Ward, B. Watson, R. C. Brunham, M. Krajden, M. Petric, D. M. Skowronski, C. Upton, and R. L. Roper.** 2003. The genome sequence of the SARS-associated coronavirus. Science **300:**1399–1404.
13. **Murray, A. W.** 2004. Recycling the cell cycle: cyclins revisited. Cell **116:**221–234.
14. **Muslin, A. J., J. W. Tanner, P. M. Allen, and A. S. Shaw.** 1996. Interaction of 14-3-3 with signaling proteins is mediated by the recognition of phosphoserine. Cell **84:**889–897.
15. **Rota, P. A., M. S. Oberste, S. S. Monroe, W. A. Nix, R. Campagnoli, J. P. Icenogle, S. Penaranda, B. Bankamp, K. Maher, M. H. Chen, S. Tong, A. Tamin, L. Lowe, M. Frace, J. L. DeRisi, Q. Chen, D. Wang, D. D. Erdman, T. C. Peret, C. Burns, T. G. Ksiazek, P. E. Rollin, A. Sanchez, S. Liffick, B. Holloway, J. Limor, K. McCaustland, M. Olsen-Rasmussen, R. Fouchier, S. Gunther, A. D. Osterhaus, C. Drosten, M. A. Pallansch, L. J. Anderson, and W. J. Bellini.** 2003. Characterization of a novel coronavirus associated with severe acute respiratory syndrome. Science **300:**1394–1399.
16. **Sambrook, J., E. F. Fritsch, and T. Maniatis. (ed.).** 1989. Molecular cloning: a laboratory manual. Cold Spring Harbor Laboratory, Cold Spring Harbor, N.Y.
17. **Singh, B. N., R. N. Mishra, P. K. Agarwal, M. Goswami, S. Nair, S. K. Sopory, and M. K. Reddy.** 2004. A pea chloroplast translation elongation factor that is regulated by abiotic factors. Biochem. Biophys. Res. Commun. **320:**523–530.
18. **Surjit, M., B. Liu, S. Jameel, V. T. K. Chow, and S. K. Lal.** 2004. The SARS coronavirus nucleocapsid (N) protein induces actin reorganization and apoptosis in COS-1 cells. Biochem. J. **383:**13–18.
19. **Surjit, M., B. Liu, P. Kumar, V. T. K. Chow, and S. K. Lal.** 2004. The nucleocapsid protein of the SARS coronavirus is capable of self-association through a C-terminal 209 amino acid interaction domain. Biochem. Biophys. Res. Commun. **317:**1030–1036.
20. **Tzivion, G., and J. Avruch.** 2002. 14-3-3 proteins: active cofactors in cellular regulation by serine/threonine phosphorylation. J. Biol. Chem. **277:**3061–3064.
21. **Vesely, J., L. Havlicek, M. Strnad, J. J. Blow, A. Donella-Deana, L. Pinna, D. S. Letham, J. Kato, L. Detivaud, and S. Leclerc.** 1994. Inhibition of cyclin-dependent kinases by purine analogues. Eur. J. Biochem. **224:**771–786.
22. **Vlahos, C. J., W. F. Matter, K. Y. Hui, and R. F. Brown.** 1994. A specific inhibitor of phosphatidylinositol 3-kinase, 2-(4-morpholinyl)-8-phenyl-4H-1-benzopyran-4-one (LY294002). J. Biol. Chem. **269:**5241–5248.
23. **Wang, X., M. Janmaat, A. Beugnet, F. E. Paulin, and C. G. Proud.** 2002. Evidence that the dephosphorylation of Ser(535) in the epsilon-subunit of eukaryotic initiation factor (eIF) 2B is insufficient for the activation of eIF2B by insulin. Biochem. J. **367:**475–481.
24. **Wang, B., K. Liu, F. T. Lin, and W. C. Lin.** 2004. A role for 14-3-3 tau in E2F1 stabilization and DNA damage-induced apoptosis. J. Biol. Chem. **279:**54140–54152.
25. **Wiertz, E. J. H., T. R. Jones, L. Sun, M. Boygo, H. J. Geuze, and H. L. Ploegh.** 1996. The human cytomegalovirus US11 gene product dislocates MHC class I heavy chains from the endoplasmic reticulum to the cytosol. Cell **84:**769–779.
26. **Wootton S.′K., R. R. Rowland, and D. Yoo.** 2002. Phosphorylation of the porcine reproductive and respiratory syndrome virus nucleocapsid protein. J. Virol. **76:**10569–10576.